OPEN ACCESS Freely available online

PLoS COMPUTATIONAL BIOLOGY

Ribavirin-Induced Anemia in Hepatitis C Virus Patients Undergoing Combination Therapy

Sheeja M. Krishnan[1], **Narendra M. Dixit**[1,2]*

1 Department of Chemical Engineering, Indian Institute of Science, Bangalore, India, **2** Bioinformatics Centre, Indian Institute of Science, Bangalore, India

Abstract

The current standard of care for hepatitis C virus (HCV) infection – combination therapy with pegylated interferon and ribavirin – elicits sustained responses in only ~50% of the patients treated. No alternatives exist for patients who do not respond to combination therapy. Addition of ribavirin substantially improves response rates to interferon and lowers relapse rates following the cessation of therapy, suggesting that increasing ribavirin exposure may further improve treatment response. A key limitation, however, is the toxic side-effect of ribavirin, hemolytic anemia, which often necessitates a reduction of ribavirin dosage and compromises treatment response. Maximizing treatment response thus requires striking a balance between the antiviral and hemolytic activities of ribavirin. Current models of viral kinetics describe the enhancement of treatment response due to ribavirin. Ribavirin-induced anemia, however, remains poorly understood and precludes rational optimization of combination therapy. Here, we develop a new mathematical model of the population dynamics of erythrocytes that quantitatively describes ribavirin-induced anemia in HCV patients. Based on the assumption that ribavirin accumulation decreases erythrocyte lifespan in a dose-dependent manner, model predictions capture several independent experimental observations of the accumulation of ribavirin in erythrocytes and the resulting decline of hemoglobin in HCV patients undergoing combination therapy, estimate the reduced erythrocyte lifespan during therapy, and describe inter-patient variations in the severity of ribavirin-induced anemia. Further, model predictions estimate the threshold ribavirin exposure beyond which anemia becomes intolerable and suggest guidelines for the usage of growth hormones, such as erythropoietin, that stimulate erythrocyte production and avert the reduction of ribavirin dosage, thereby improving treatment response. Our model thus facilitates, in conjunction with models of viral kinetics, the rational identification of treatment protocols that maximize treatment response while curtailing side effects.

Citation: Krishnan SM, Dixit NM (2011) Ribavirin-Induced Anemia in Hepatitis C Virus Patients Undergoing Combination Therapy. PLoS Comput Biol 7(2): e1001072. doi:10.1371/journal.pcbi.1001072

Editor: Rustom Antia, Emory University, United States of America

Received August 30, 2010; **Accepted** December 29, 2010; **Published** February 3, 2011

Funding: This work was supported by the Department of Biotechnology Centre of Excellence for Research on Hepatitis C Virus, India. The funders had no role in study design, data collection and analysis, decision to publish, or preparation of the manuscript.

Competing Interests: The authors have declared that no competing interests exist.

* E-mail: narendra@chemeng.iisc.ernet.in

Introduction

130–170 million people worldwide are currently infected with hepatitis C virus (HCV) [1]. Over 70% of HCV infections become chronic and if untreated may lead to cirrhosis and hepatocellular carcinoma, necessitating liver transplantation [1]. The standard of care for HCV infection involves combination therapy with pegylated interferon and ribavirin [2]. Ribavirin alone does not elicit a lasting antiviral response [3–6], yet it substantially improves treatment response in combination with interferon [7–11]. For instance, whereas ~29% of the patients treated with interferon exhibited a sustained virological response (SVR), the response rate increased to ~56% upon addition of ribavirin [8]. Ribavirin, however, is associated with the side-effect, hemolytic anemia, which often renders therapy intolerable [4,12–15]. With the standard ribavirin dosage of 1000–1200 mg/day, 54% of the patients treated experienced a decline in the hemoglobin (Hb) level of over 3 g/dL, and 10% of the men and 7% of the women treated experienced an Hb decline of over 5 g/dL (normal Hb range: 14–16 g/dL) [15]. This drop in Hb often necessitates a reduction of ribavirin dosage, which significantly compromises treatment response [7,13,14,16]. The probability of achieving SVR is estimated to decrease from ~65% to ~45% when ribavirin dosage is reduced from ~15 mg/kg to ~7 mg/kg of body weight, in combination with pegylated interferon at 1.5 μg/kg of body weight [7]. Patients receiving fewer than 60% of the planned ribavirin doses had lower response rates [14], indicating that lower cumulative ribavirin exposure results in poorer treatment response [13,16]. The rates of relapse of infection following the end of treatment also increased upon lowering ribavirin dosage [14,16]. In a recent clinical trial where interferon was employed with telaprevir, a promising new inhibitor of HCV protease, response rates were lowest in patients who were not administered ribavirin [17], underscoring the importance of ribavirin in achieving SVR.

Alternatives for patients who do not respond to combination therapy do not exist yet [2,18]. Significant efforts are underway therefore to identify treatment protocols that maximize response rates to combination therapy while curtailing side-effects [16,19–25]. A particularly promising strategy is to supplement combination therapy with growth hormones, such as erythropoietin, that stimulate erythropoiesis and thus avert the reduction of ribavirin dosage, potentially improving treatment response [26–31]. The predominant mechanism(s) of the anti-HCV activity of ribavirin remain to be established [32–34]. Mathematical models of viral kinetics have been developed that describe the antiviral activity of interferon and the enhancement of treatment response rates due to

Author Summary

The treatment of HCV infection poses a major global health-care challenge today. The current standard of care, combination therapy with interferon and ribavirin, works in only about half of the patients treated. Because no alternatives are available yet for patients in whom combination therapy fails, identifying ways to improve response to combination therapy is critical. Increasing exposure to ribavirin does improve response but is associated with the severe side-effect, anemia. One way to maximize treatment response therefore is to increase ribavirin exposure to levels just below where anemia becomes intolerable. A second way is to supplement combination therapy with growth hormones, such as erythropoietin, that increase the production of red blood cells (erythrocytes) and compensate for ribavirin-induced anemia. Rational optimization of combination therapy thus relies on a quantitative description of ribavirin-induced anemia, which is currently lacking. Here, we develop a model of the population dynamics of erythrocytes in individuals exposed to ribavirin that quantitatively describes ribavirin-induced anemia. Model predictions capture several independent observations of ribavirin-induced anemia in HCV patients undergoing combination therapy, estimate the threshold ribavirin exposure beyond which anemia becomes intolerable, suggest guidelines for the usage of growth hormones, and facilitate rational optimization of therapy.

ribavirin, and are being extended to predict the impact of new antiviral drugs [34–42]. Ribavirin-induced anemia, on the other hand, remains poorly understood [13,24,25,43–47] and precludes rational optimization of combination therapy.

Here, we construct a mathematical model of the population dynamics of erythrocytes that quantitatively describes ribavirin-induced anemia and informs future strategies for improving outcomes of combination therapy. Model predictions capture experimental observations of the accumulation of ribavirin in erythrocytes and the ensuing Hb decline in HCV patients following the onset of combination therapy, estimate the enhanced turnover rate of erythrocytes during therapy and the threshold ribavirin exposure beyond which anemia is intolerable, present guidelines for the optimal usage of growth hormone supplements, and provide a framework, in conjunction with models of viral kinetics, for rational optimization of combination therapy.

Results

Model formulation

Prior to the onset of treatment with ribavirin, the population of erythrocytes (RBCs) in an HCV infected individual is constant; a balance exists between RBC production and death (Fig. 1). Following the onset of treatment, ribavirin administered orally gets rapidly transported from the plasma to RBCs, where it is phosphorylated to its mono-, di- and tri-phosphate analogs (RMP, RDP, and RTP) [48]. Phosphorylated analogs are neither easily metabolized nor transported out of RBCs [48]. Consequently, ribavirin accumulates inside RBCs in the form of its phosphorylated analogs; the total intracellular concentration of ribavirin can be >100-fold its extracellular concentration [47]. This dramatic accumulation of ribavirin may induce oxidative damage and result in enhanced extra vascular death of RBCs [12]. Indeed, RBC lifespan decreased from 107 ± 22 d in HCV patients not exposed to ribavirin to 39 ± 13 d in HCV patients undergoing

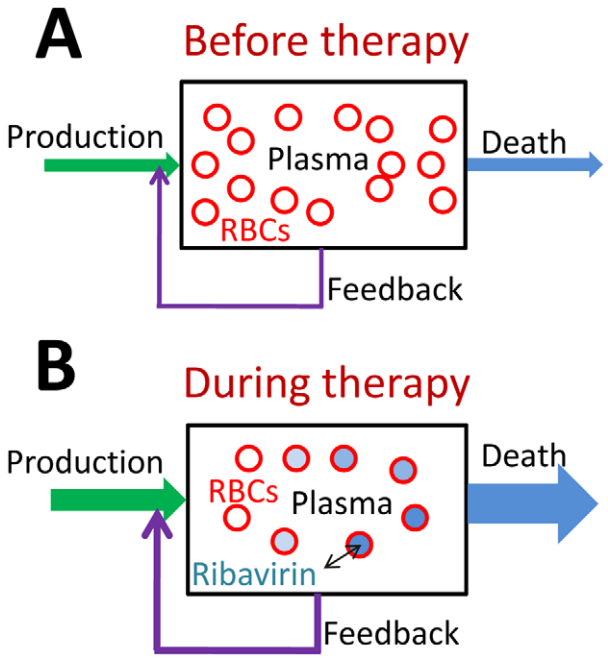

Figure 1. Schematic of the population dynamics of RBCs in HCV infected individuals. A, Before the onset of combination therapy, the production and death rates of RBCs are balanced and the population of RBCs in plasma is constant. **B**, Following the onset of therapy, ribavirin enters RBCs and increases their death rates. Cells born at different times are exposed to ribavirin for different durations and hence carry different concentrations of ribavirin. The enhanced death rate lowers the RBC population, which triggers an increase in the RBC production from the bone marrow by a negative feedback through the hormone erythropoietin.
doi:10.1371/journal.pcbi.1001072.g001

treatment with ribavirin [49,50]. The shortened RBC lifespan creates an imbalance between RBC production and death and results in a decline in the RBC population. Accordingly, Hb levels drop and patients become anemic. We construct a mathematical model to describe this dynamics of ribavirin-induced anemia (Methods).

Model predictions

Population dynamics of RBCs during treatment with ribavirin. We present model predictions in terms of the cumulative population, $m(C,t)$, which is the population of RBCs at time t following the onset of treatment in which the concentration of ribavirin phosphorylated analogs, RXP, is less than or equal to C (Fig. 2A). (RXP comprises RMP, RDP, and RTP.) At the start of treatment ($t=0$), no cells contain RXP, and $m(C,0)=N_0$ for all C, where N_0 is the steady population of RBCs prior to the onset of treatment. In other words, the population of cells carrying RXP at concentrations smaller than or equal to C is N_0 for all $C\geq 0$. At $t=0$, the production and death rates of RBCs are in balance (Fig. 2B), the hemoglobin level, $Hb=Hb_0$, and the average intracellular concentration of ribavirin, $C_{avg}=0$ (Fig. 2C). With time, ribavirin accumulates inside cells. At any time $t>0$, a distribution of RXP concentrations across cells emerges with cells exposed to ribavirin longer possessing higher concentrations of RXP. Thus, cells present from the start of treatment possess the highest concentration of RXP. At $t=1$ d, for instance, the latter cells possess RXP at the concentration $C\approx 0.04C_{\max}$, where $C_{\max}=k_pC_p^{\max}/k_d$ is the maximum intracellular concentration of

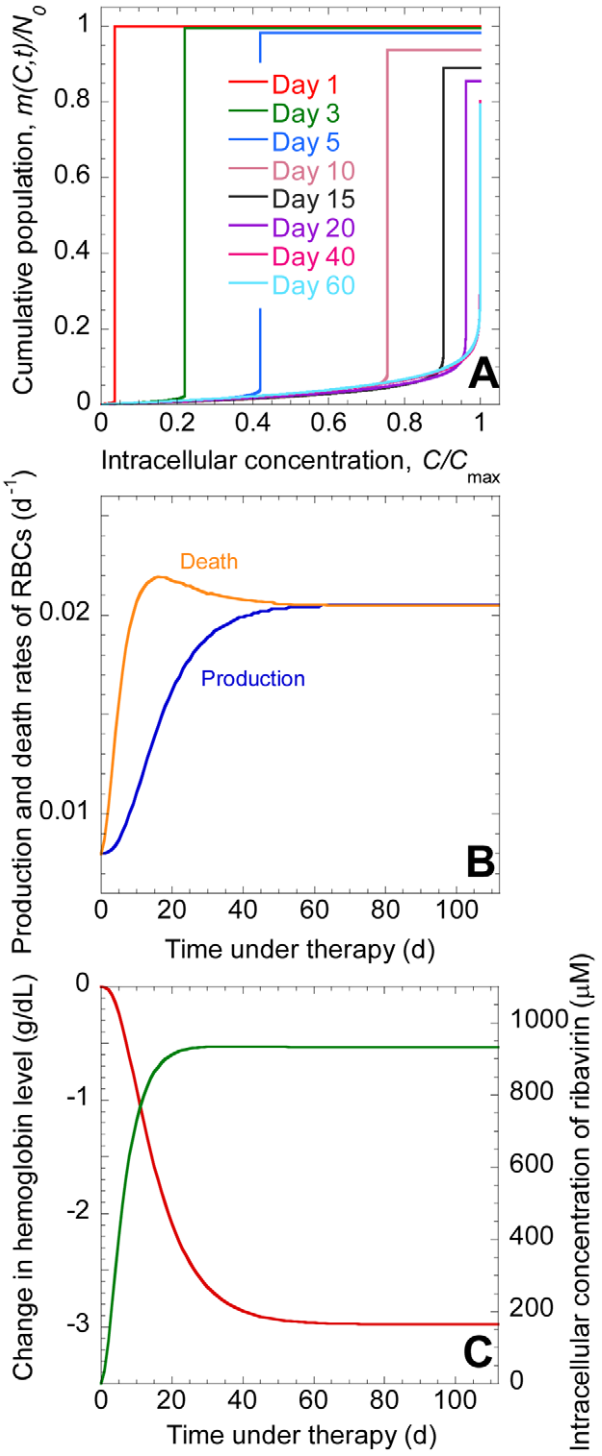

Figure 2. Model predictions of the dynamics of ribavirin-induced anemia. A, The cumulative population, $m(C,t)$, of RBCs as a function of the intracellular concentration of RXP, C, at different times, t, following the onset of combination therapy, predicted by Eqs. (1)–(3). Parameters employed are listed in Table 1. $m(C,t)$ is normalized by N_0 and C by $C_{\max}=k_pC_p^{\max}/k_d$. **B**, The production rate, $P(t)$, and the death rate $\int_0^\infty n(C,t)D(C)dC$ of RBCs. **C**, The corresponding change in Hb (red) and C_{avg} (green).
doi:10.1371/journal.pcbi.1001072.g002

RXP for a given extracellular concentration of ribavirin $C_p^{\max}$ (Fig. 2A). Cells born after the onset of treatment possess RXP at concentrations smaller than $\approx 0.04C_{\max}$ at $t=1$ d. Because most of the cells present at $t=1$ d are from the population that existed at the start of therapy, $m(C,t)$ exhibits a sharp rise at $C\approx 0.04C_{\max}$ and reaches the value $\mathcal{N}(t=1)$ (Fig. 2A). With time, the sharp rise in $m(C,t)$ shifts to higher values of C (Fig. 2A) indicating greater accumulation of RXP. Accordingly, C_{avg} increases (Fig. 2C). Cells die at increasing rates as intracellular RXP accumulates (Fig. 2B). The population of RBCs, $\mathcal{N}(t)$, and, hence, Hb correspondingly decrease (Fig. 2C). New cells are continuously produced at a rate that increases as the RBC population declines (Fig. 2B). Eventually, a new balance between RBC production and death is attained, $m(C,t)$ reaches a steady distribution, C_{avg} reaches an asymptotic maximum C_{avg}^{∞}, and Hb attains a new, lower steady value Hb_{∞}.

Factors that influence the severity of ribavirin-induced anemia. An increase in the steady state plasma concentration of ribavirin, $C_p^{\max}$, which may be achieved with a higher dosage, results in an increase in C_{avg}^{∞} and a decrease in Hb_{∞}, illustrating the more severe anemia that results with increased ribavirin exposure. For instance, increasing $C_p^{\max}$ from 5 μM to 15 μM increases the total drop in Hb, $\Delta Hb=Hb_0-Hb_{\infty}$, from ~2 g/dL to ~5 g/dL (Fig. 3A). An increase in the intracellular phosphorylation rate, k_p, (or a decrease in the loss rate of intracellular RXP, k_d) results in a higher C_{avg}^{∞} for the same $C_p^{\max}$, which in turn elevates cell death rates and lowers Hb_{∞}. Thus, ΔHb increases from ~2.5 g/dL when $k_p=50$ d^{-1} to ~3.5 g/dL when $k_p=80$ d^{-1} (Fig. 3B), illustrating that differences in the intracellular metabolism of ribavirin may contribute to inter-patient variations in the severity of ribavirin-induced anemia. Enhancing the RBC production rate, by increasing $P_{\max}$ (see Eq. (3)), (or lowering the sensitivity of the RBC death rate to ribavirin accumulation, by increasing C_{50} or decreasing γ (see Eq. (2))), reduces ΔHb (Fig. 3C). Administration of growth hormones, such as erythropoietin, enhances the RBC production rate, which reduces ΔHb for the same ribavirin exposure and thus improves the tolerability of ribavirin. Similarly, decrease in the intracellular inosine triphosphatase level, observed recently in some patients [51], may interfere with RTP activity and lower the sensitivity of the RBC death rate to ribavirin, which also reduces ΔHb and improves the tolerability of ribavirin.

Inter-patient variations. Inter-patient variability in the severity of anemia may arise from variations in the intracellular uptake, accumulation, or metabolism of ribavirin, as well as in the dependence of the RBC lifespan on ribavirin accumulation and in the sensitivity of the RBC production rate to changes in Hb. To obtain a measure of this inter-patient variability, we calculated ΔHb using 500 different combinations of the values of the parameters, k_p, k_d, C_{50} and γ, for a range of values of $C_p^{\max}$. The parameter values for each combination were chosen randomly from Gaussian distributions based on the mean values and confidence levels of the respective parameters obtained from comparisons of our model predictions with patient data (see below). Indeed, we find that inter-patient variations in ΔHb may be substantial for any ribavirin exposure (Fig. 4A) or intracellular accumulation (Fig. 4B). Further, the variation increases with increase in ribavirin exposure and intracellular accumulation.

Below, we compare our model predictions with experiments.

Comparisons of model predictions with patient data

We consider a recent study of the time-evolution of C_{avg} and Hb in 19 Japanese patients following the onset of combination therapy [47]. In this latter study, no reduction of ribavirin dosage is

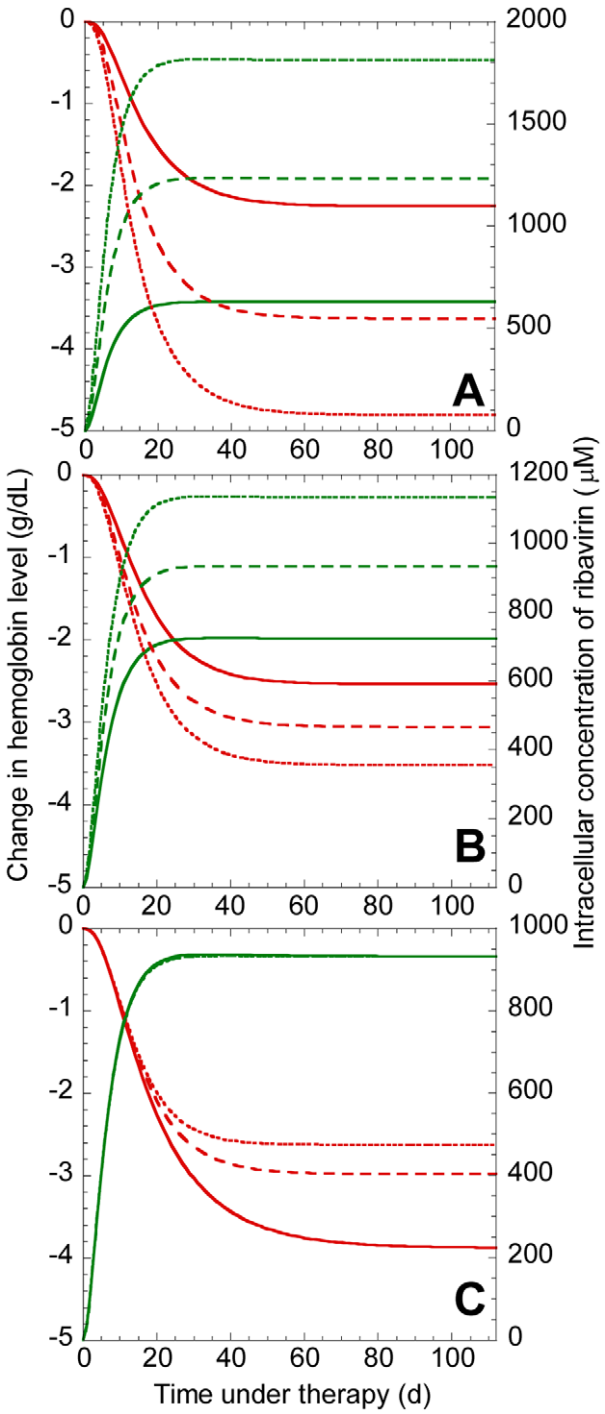

Figure 3. Factors influencing the dynamics of ribavirin-induced anemia. Changes in *Hb* (red) and C_{avg} (green) predicted by Eqs. (1)–(3) for different parameter values: **A**, $C_p^{max} = 5$ μM (solid lines), 10 μM (dashed lines) and 15 μM (dotted lines). **B**, $k_p = 50\,d^{-1}$ (solid lines), $65\,d^{-1}$ (dashed lines), $80\,d^{-1}$ (dotted lines). **C**, $P_{max} = 5.4 \times 10^{11}$ cells d^{-1} (solid lines), 8.3×10^{11} cells d^{-1} (dashed lines), 1.1×10^{12} cells d^{-1} (dotted lines). The other parameters are mentioned in Table 1.

doi:10.1371/journal.pcbi.1001072.g003

reported. The patients were divided into two groups based on whether $C_{avg}^{\infty} < 1000$ μM (7 patients) or $C_{avg}^{\infty} > 1000$ μM (12 patients); the data are reported as the average within each group. We fit model predictions of C_{avg} and *Hb* to the data of the former 7 patients using k_p, k_d, C_{50} and γ as adjustable parameters. (Interferon may also induce anemia, but does so to a much smaller extent than ribavirin [13]. We therefore assume that the *Hb* decline in patients undergoing combination therapy is primarily due to ribavirin.) We fix the remaining parameters based on previous studies or from analysis of independent experiments (Methods). Model predictions provide good fits to the data and yield estimates of k_p, k_d, C_{50} and γ (Fig. 5A). The fits suggest that our model is able to describe the underlying dynamics of ribavirin-induced anemia in HCV patients.

Interestingly, with the same parameter values, our model captures changes in *Hb* and C_{avg} from the other 12 Japanese patients, as well as an independent data set of *Hb* decline in another group of HCV patients undergoing combination therapy [29] (Fig. 5B), validating our best-fit parameter estimates. Further, with the same parameter values, we estimate that the RBC lifespan is 38 days (95% CI: 19–55 days) in Japanese patients with $C_{avg}^{\infty} < 1000$ μM and 33 days (95% CI: 14–53 days) in Japanese patients with $C_{avg}^{\infty} > 1000$ μM. These estimates of the RBC lifespan are in close agreement with independent estimates, 39 ± 13 days, from measurements of alveolar carbon monoxide [49,50], presenting another successful test of our model. Finally, we find that our predictions of the dependence of ΔHb on C_p^{max} and C_{avg}^{∞} using the same parameters above are also in agreement with observations in the Japanese patients [47] (Fig. 5C,D). Our model thus presents a robust description of ribavirin-induced anemia in HCV patients undergoing combination therapy.

Clinical implications

Our model has several clinical implications. First, it enables estimation of the threshold ribavirin exposure beyond which anemia is intolerable. Current treatment guidelines recommend a reduction of ribavirin dosage when *Hb* decreases below 10 g/dL. We apply our model to predict Hb_{∞} as a function of C_p^{max}. We find that on average (when $Hb_0 = 14.4$ g/dL) $Hb_{\infty} < 10$ g/dL when $C_p^{max} > 13$ μM (Fig. 6A). Thus, steady state plasma concentrations above 13 μM would render ribavirin therapy intolerable. While the dependence of the peak plasma concentration on dosage following a single ribavirin dose has been determined [48], the dependence of C_p^{max} on dosage remains to be established. A description of the multiple dose pharmacokinetics of ribavirin, which also remains elusive [6,34,48,52,53], would establish the dosage corresponding to C_p^{max} of 13 μM that would render ribavirin intolerable.

Second, when C_p^{max} is above the threshold, our model allows estimation of the increase in RBC production, which may be achieved by administration of exogenous growth hormones such as recombinant erythropoietin, necessary to avert the currently recommended reduction of dosage. Because growth hormones also have side-effects [29,54], one strategy is to use them at levels just enough to increase Hb_{∞} to 10–12 g/dL (rather than the pretreatment level), which renders ribavirin tolerable [16]. We apply our model to predict the level of RBC production necessary for achieving Hb_{∞} of 10–12 g/dL for different values of C_p^{max} (Fig. 6B). Thus, when $C_p^{max} = 15$ μM, RBC production rates of 8.44 and 10.2 million cells s^{-1} are necessary for ensuring Hb_{∞} of 10 and 12 g/dL, respectively. Increase in endogenous erythropoietin levels during therapy, also observed experimentally [45,55], results in an enhanced production rate of 8.1 million cells s^{-1}, which is 3.5-fold higher than the basal production rate (here 2.3 million cells s^{-1} in the absence of ribavirin) but inadequate to achieve the desired Hb_{∞}. Hormone supplements may be employed to provide the balance of 0.34 or 2.1 million cells s^{-1}

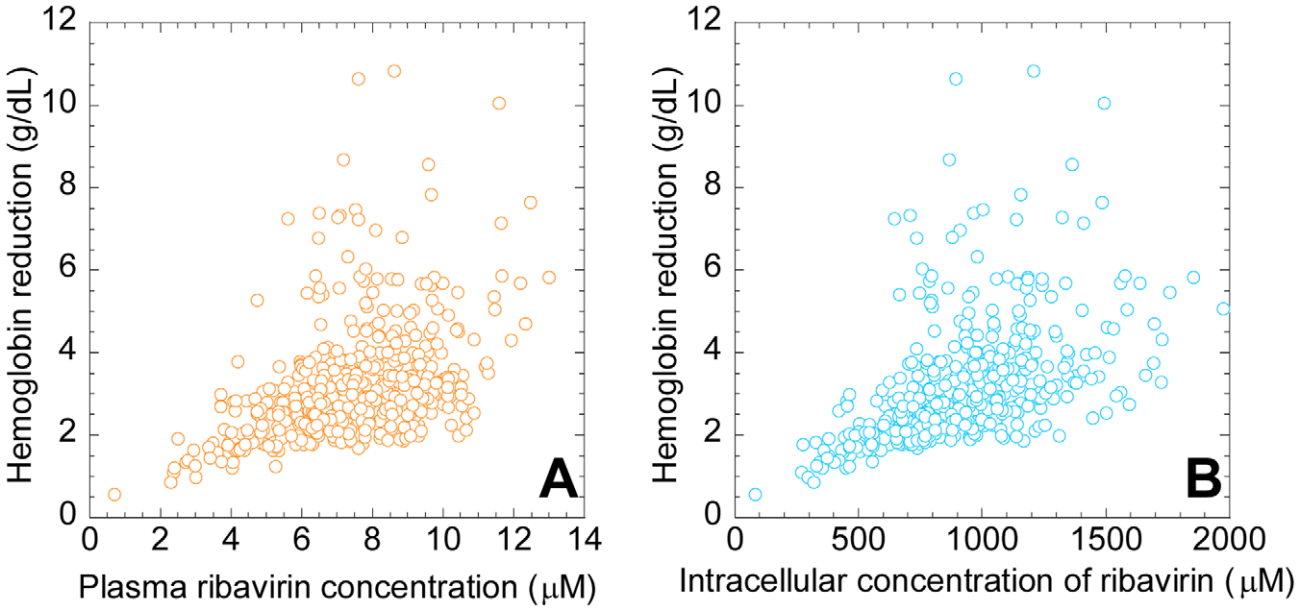

Figure 4. Model predictions of the variations in the severity of ribavirin-induced anemia. The reduction in Hb ($\Delta Hb = Hb_0 - Hb_\infty$) predicted by Eqs. (1)–(3) as a function of **A**, $C_p^{\max}$, and **B**, C_{avg}^{∞}, for 500 different combinations of the parameter values (mean±s.d.) $C_p^{\max}(7.5\pm1.9\,\mu M)$, $k_p(65\pm8\,d^{-1})$, $k_d(0.5\pm0.07\,d^{-1})$, $C_{50}(408\pm98\,\mu M)$, and $\gamma(1\pm0.35)$. The standard deviations on the parameter values correspond to the 95% confidence limits obtained from the best-fits to patient data (see Fig. 5). The other parameters are mentioned in Table 1.
doi:10.1371/journal.pcbi.1001072.g004

increase in the RBC production rate to ensure Hb_∞ of 10 or 12 g/dL, respectively. This deficiency in RBC production that hormone supplements must compensate increases with ribavirin exposure (Fig. 6B).

Discussion

The ability to enhance treatment response rates renders ribavirin central to the treatment of HCV infection. Maximizing the benefit of ribavirin to patients requires striking the right balance between its antiviral activity and its treatment-limiting side-effect, hemolytic anemia. Rational approaches to therapy optimization thus rely on quantitative descriptions of both the antiviral and the hemolytic activities of ribavirin. Extant mathematical models predict the enhancement in treatment response due to ribavirin [34–42]. Ribavirin-induced anemia, however, remains poorly described and limits our ability to maximize treatment response. Here, we fill this gap by constructing a model of the population dynamics of RBCs that quantitatively describes ribavirin-induced anemia. By assuming that intracellular accumulation of ribavirin enhances RBC death rate in a dose-dependent manner, our model captures several independent observations of ribavirin-induced anemia in HCV patients undergoing combination therapy. In particular, our model predicts the dynamics of the accumulation of ribavirin in RBCs and the resulting decline of Hb in patients following the onset of therapy, estimates the reduced lifespan of RBCs during therapy, and describes inter-patient variations in the severity of anemia, thus presenting a robust description of ribavirin-induced anemia, which, in conjunction with models of viral kinetics, may facilitate identification of treatment protocols that maximize the impact of ribavirin in the treatment of HCV infection.

Our model has clinical implications. First, it allows estimation of the threshold ribavirin exposure beyond which ribavirin-induced anemia becomes intolerable. For instance, with model parameters that describe ribavirin-induced anemia in the patients we considered (Fig. 5), we estimate that steady state plasma ribavirin concentrations above 13 μM would render ribavirin therapy intolerable. Determining dosage levels corresponding to this steady state plasma concentration requires knowledge of the pharmacokinetics of ribavirin, which is currently lacking [6,34,48,52,53]. Ribavirin pharmacokinetics is peculiar because of an unusually long elimination phase that follows rapid absorption and distribution phases upon oral dosing [48]. Standard absorption-elimination models of drug pharmacokinetics are unable to describe this long elimination phase. Models that include additional compartments have been proposed to capture the three-phase pharmacokinetics of ribavirin [52], but the biological origin of these compartments remains unclear. An additional complication is that the half-life of the elimination phase increases from 79 h following a single dose to 274–298 h following multiple dosing [48], suggesting that parameters that describe single dose pharmacokinetics may not apply to multiple dose pharmacokinetics. In the absence of rigorous models of ribavirin pharmacokinetics, one may have to rely on empirical relationships between the dosage and the resulting steady state plasma concentration following multiple dosing (e.g., [56]) to establish the dosage that would ensure tolerability of ribavirin while maximizing treatment response.

Second, our model suggests guidelines for the usage of hormone supplements, such as erythropoietin, which enhance RBC production and improve the tolerability of ribavirin. For instance, we predict that when ribavirin accumulates to a plasma concentration of 15 μM, the associated enhanced RBC death rate elicits a natural response that increases RBC production 3.5-fold, from 2.3 to 8.1 million cells s^{-1}. This response, however, is inadequate to suppress ribavirin-induced anemia adequately and renders ribavirin intolerable. We estimate then that growth hormone supplements must increase RBC production rate by an additional 0.34–2.1 million cells s^{-1} to render ribavirin tolerable. This compensation that hormone supplements must provide increases with ribavirin accumulation. Identifying the dosage of

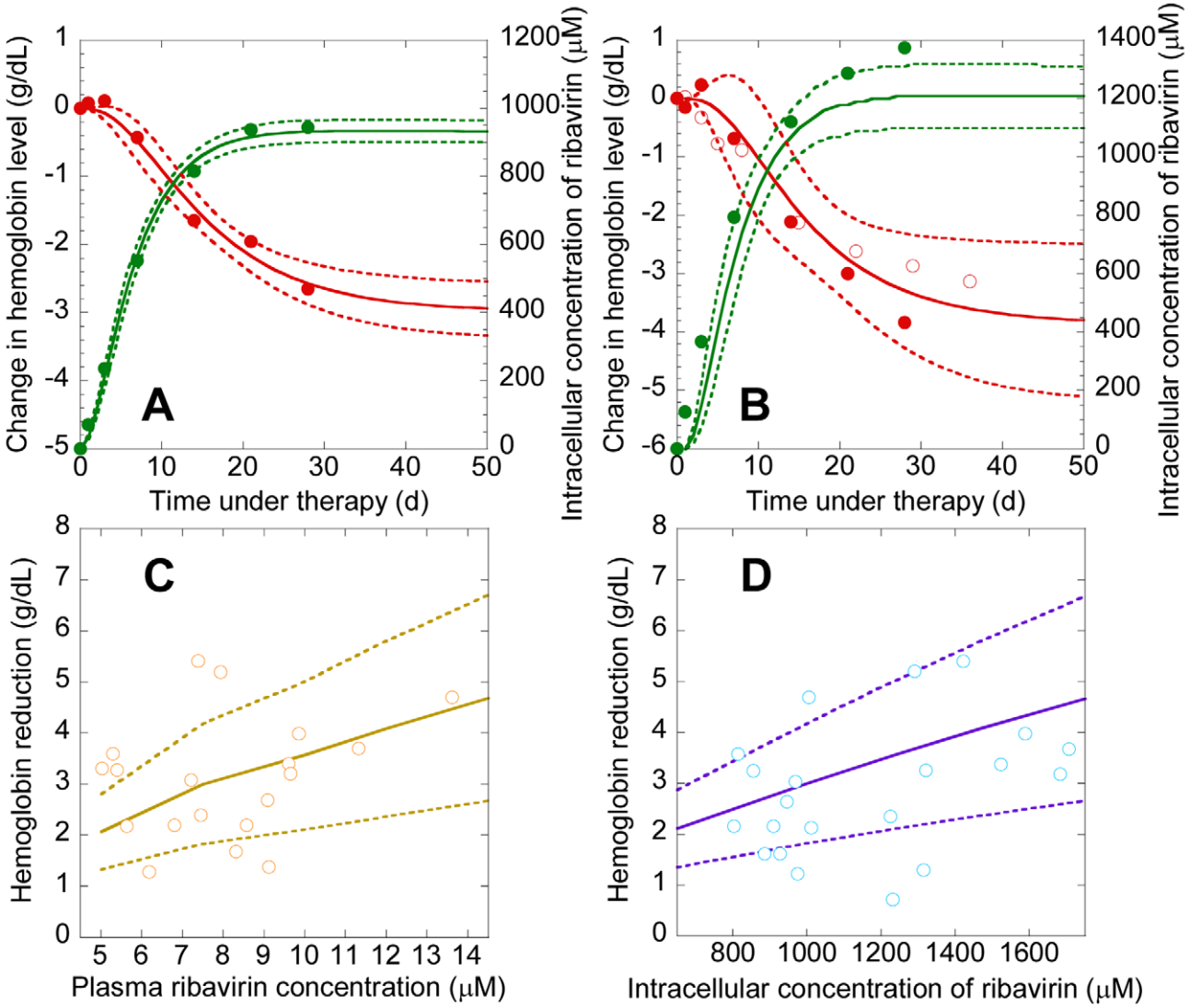

Figure 5. Comparisons of model predictions with experiments. A, Best-fits of model predictions (lines) of *Hb* (red) and C_{avg} (green) with experimental data (symbols) from 7 Japanese patients with $C_{avg}^{\infty}<1000$ μM [47]. We let $Hb_0=14.4$ g/dL and $C_p^{\max}=7.5\,\mu M$ following the mean reported values for these patients [47]. We use k_p, k_d, C_{50}, and γ as adjustable parameters. The remaining parameters are mentioned in Table 1. The resulting best-fit parameter estimates (95% CI) are $k_p=65\,d^{-1}(47-84\,d^{-1})$, $k_d=0.5\,d^{-1}(0.3-0.7\,d^{-1})$, $C_{50}=408\,\mu M(189-628\,\mu M)$, and $\gamma=1(0.2-1.8)$. Dashed lines show 95% confidence intervals on the predictions. **B**, Comparisons of our predictions (lines) of *Hb* (red) and C_{avg} (green) using the parameters above with data (symbols) from 12 Japanese patients with $C_{avg}^{\infty}>1000$ μM (solid circles) [47]. In the latter patients, the mean $Hb_0\approx15$ g/dL and $C_p^{\max}=9.8\,\mu M$. We also show comparisons with independent data from 20 patients [29] (open circles) with mean $Hb_0=15.1$ g/dL. Solid lines are predictions with $Hb_0=15.1$ g/dL and $C_p^{\max}=9.8\,\mu M$, and the mean parameters mentioned above, and dashed lines represent standard deviations. **C**, **D**, Model predictions (lines) and experimental observations (symbols) of the reduction in *Hb* ($\Delta Hb=Hb_0-Hb_{\infty}$) under combination therapy as a function of **C**, $C_p^{\max}$, and **D**, C_{avg}^{∞}, in 19 Japanese patients [47]. Solid lines represent predictions with the mean parameter values above and dashed lines represent standard deviations obtained from several hundred realizations of our model predictions for different combinations of the values of k_p, k_d, C_{50}, and γ generated randomly from distributions based on the best-fit parameter estimates and 95% confidence limits mentioned above.
doi:10.1371/journal.pcbi.1001072.g005

the growth hormones that induces the necessary RBC production requires knowledge of the dose-response relationships and of the pharmacokinetics of the growth hormones, which are yet to be fully elucidated [26–31].

Third, genetic variations that resulted in a deficiency in the enzyme inosine triphosphatase (ITPA) were recently found to protect HCV patients against ribavirin-induced anemia [51]. Deficiency in ITPA causes an increase in inosine triphosphate levels in RBCs, which is thought to interfere with RTP activity and thereby suppress the hemolytic potential of ribavirin. Because deficiency in ITPA is a clinically benign condition, therapeutic intervention to suppress ITPA presents a promising new strategy to curtail ribavirin-induced anemia without compromising the antiviral activity of ribavirin [51]. Our model may be adapted to inform the development of such an intervention strategy. In our model, the dependence of the death rate of RBCs on ribavirin accumulation, determined by Eq. (2) (Methods), would now be a function of the ITPA level. Thus, experiments that determine how variations in the ITPA level both in the absence and in the presence of ribavirin influence RBC lifespan would provide the

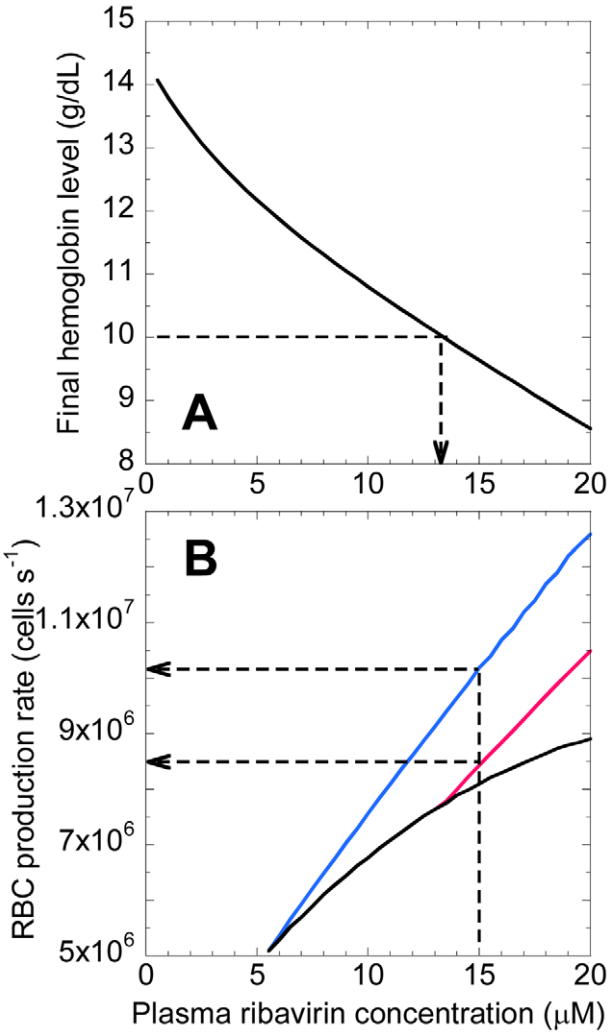

Figure 6. Model predictions of threshold ribavirin exposure and requisite RBC production. A, Prediction of Hb_∞ as a function of $C_p^{\max}$. The arrow indicates the threshold $C_p^{\max}$ above which $Hb_\infty < 10$ g/dL. **B**, Predictions of the RBC production rate during therapy (black) and the production rate required to maintain Hb_∞ of 10 g/dL (pink) and 12 g/dL (blue) as functions of $C_p^{\max}$. The arrows indicate the desired production rates when $C_p^{\max} = 15\,\mu$M. Parameter values employed are mentioned in Table 1.
doi:10.1371/journal.pcbi.1001072.g006

necessary inputs for our model to account explicitly for the role of ITPA in ribavirin-induced anemia. The resulting model would enable determination of the minimal inhibition of ITPA necessary to maintain ribavirin-induced anemia within tolerable limits. Conversely, using information of the ITPA level intrinsic to a patient, the model can be applied to predict the maximum ribavirin dosage that the patient can tolerate, thus presenting an avenue for personalizing the treatment of HCV infection.

Methods

Model development

We consider the RBC population in an individual at time t following the onset of treatment with ribavirin ($t=0$) (Fig. 1). RBCs produced at different times in the interval from 0 to t will have been exposed to ribavirin for different durations and accordingly have different intracellular levels of ribavirin. We define $n(C,t)\Delta C$ as the population of RBCs that contain ribavirin phosphorylated analogs, RXP, which comprises RMP, RDP, and RTP, at concentrations between C and $C+\Delta C$ at time t. $n(C,t)$ is thus the number density of RBCs containing RXP at concentration C at time t. The time evolution of $n(C,t)$ is governed by the following equation (Text S1)

$$\frac{\partial}{\partial t}n(C,t) = -\frac{\partial}{\partial C}[Q(C,C_c)n(C,t)] - n(C,t)D(C) \qquad (1)$$

The first term on the right-hand-side in Eq. (1) represents the change in $n(C,t)$ due to intracellular phosphorylation of ribavirin. $Q(C,C_c) = k_p C_c - k_d C$ is the net rate of increase of C due to phosphorylation, C_c is the intracellular concentration of (unphosphorylated) ribavirin, k_p is the phosphorylation rate and k_d is the rate of loss, including by possible slow dephosphorylation, of RXP. In vitro studies of ribavirin uptake by RBCs observe rapid (<10 min) equilibration of intracellular and extracellular ribavirin [53,57]. We assume therefore that $C_c(t) \approx C_p(t)$, the concentration of ribavirin in plasma. With twice daily oral administration of ribavirin, C_p rises from zero at $t=0$ and reaches an asymptotic maximum, $C_p^{\max}$, so that $C_p(t) = C_p^{\max}(1-\exp(-t/t_a))$, where t_a is the characteristic timescale of the accumulation of ribavirin in plasma [6,38].

The second term on the right-hand side of Eq. (1) accounts for the loss of RBCs due to their death. We assume that the death rate, D, of RBCs increases with C as follows

$$D(C) = D_0\left(1+\left(\frac{C}{C_{50}}\right)^{\gamma}\right) \qquad (2)$$

where D_0 is the death rate of RBCs in the absence of ribavirin, C_{50} is that value of C at which the death rate doubles (or the lifespan halves) compared to that in the absence of ribavirin, and γ, analogous to the Hill coefficient, determines the sensitivity of D to changes in C. (A saturable form for $D(C)$ appears inconsistent with available data; see Text S2, Fig. S1.)

Equation (1) is constrained by the initial condition that $C=0$ in all cells at the start of therapy, so that $n(C,0) = N_0\delta(C)$, where N_0 is the population of RBCs at $t=0$, and $\delta(C)$ is the Dirac delta function, which satisfies $\delta(C\neq 0)=0$ and $\int_{-\infty}^{\infty}\delta(C)dC = 1$. In other words, the Dirac delta function ensures that no cells have RXP at non-zero concentrations at $t=0$. A second constraint on Eq. (1) is imposed by the boundary condition that when $t>0$, newborn cells contain no RXP so that $n(0,t) = P(t)/Q(0,C_c)$ (Text S1) where

$$P(t) = \frac{P_{\max}\theta^b}{\theta^b + \left(\frac{N(t)}{V}\right)^b} \qquad (3)$$

is the rate of production of RBCs at time t.

The production of RBCs by the bone marrow is regulated by a negative feedback mechanism involving the hormone erythropoietin [58]. Recent studies on modeling erythropoiesis elucidate the complexities involved in a quantitative description of this feedback mechanism [59–65]. Here, we employ Eq. (3) to capture the essential features of this negative feedback: As the population of RBCs, $N(t) = \int_0^{\infty} n(C,t)dC$, decreases, P increases. $P_{\max}$ is the maximum production rate of RBCs, which occurs when N is

vanishingly small, θ is that value of the RBC population per unit volume of blood (N/V) at which $P=P_{\max}/2$, V is the volume of blood, and b, analogous to the Hill coefficient, determines the sensitivity of P to changes in N/V. Eq. (3) provides good fits to independent measurements of the dynamics of the recovery of RBCs following phlebotomy (Text S3, Fig. S2).

Equations (1)–(3) present a model of the population dynamics of RBCs in individuals undergoing treatment with ribavirin. We solve the equations (see below) and obtain the population density, $n(C,t)$, and the corresponding cumulative population, $m(C,t)=\int_0^C n(C',t)dC'$, using which we predict the time-evolution of the hemoglobin level in blood, $Hb(t)=\frac{100}{3}\frac{v_e}{V}N(t)$ (where v_e is the volume of a single erythrocyte); the average concentration of ribavirin in RBCs, $C_{avg}(t)=\frac{1}{N(t)}\int_0^\infty n(C,t)(C+C_c)dC$; and the average RBC lifespan, $1/D_{avg}$, where $D_{avg}(t)=\frac{1}{N(t)}\int_0^\infty n(C,t)D(C)dC$ is the average death rate of RBCs.

Solution of model equations using the method of characteristics

Equation (1) along with the initial and boundary conditions is equivalent to the following set of differential equations obtained using the method of characteristics (Text S4)

$$\begin{aligned} &dS_i(t)/dt = -D(C_i)S_i(t)\\ &S_i(t_i)=\begin{cases} N_0 & i=0\\ P(t_i)\Delta t & i=1,2,3,\ldots\end{cases}\\ &dC_i(t)/dt = k_pC_c(t)-k_dC_i(t)\\ &C_i(t_i)=0\end{aligned} \qquad (4)$$

where $S_i(t)$ is the subpopulation of cells born within an interval Δt of $t_i=i\Delta t$ that survive at time t. $C_i(t)$ is the concentration of RXP in the latter cells at time t. We solve Eq. (4) along with Eqs. (2) and (3) with $\Delta t=0.01$ d using a program written in MATLAB (Text S5). We validate our solution methodology against an analytical solution that can be obtained in the limiting case when the RBC death rate is independent of RXP accumulation (Text S6, Fig. S3). We also ensure that $\Delta t=0.01$ d allows accurate integration of Eq. (4) without compromising computational efficiency (Fig. S4). From the solution, we calculate the quantities of interest, viz., $m(C,t)=\sum_{i\in\{C_i\le C\}} S_i(t)$, $N(t)=\sum_i S_i(t)$, $C_{avg}(t)=C_c(t)+\frac{1}{N(t)}\sum_i C_i(t)S_i(t)$, and $D_{avg}(t)=\frac{1}{N(t)}\sum_i D(C_i(t))S_i(t)$.

Model parameters

We employ the following values of the model parameters unless stated otherwise. The average RBC lifespan in normal man is ~120 days [49,66], which corresponds to $D_0=0.0083\ \mathrm{d}^{-1}$. We let $b=7$ following earlier studies [59] and obtain $P_{\max}=8.4\times10^{12}$ cells d^{-1} from an independent analysis of blood loss experiments (Text S3). We fix $V=5\ \mathrm{L}$ and $v_e=9\times10^{-14}\ \mathrm{L}$ [67]. Using $Hb_0=14.4\ \mathrm{g/dL}$ [47], we get $N_0=2.4\times10^{13}$ cells. We obtain θ from the initial steady state $P(0)=D_0N_0$. Further, we let $C_p^{\max}=7.5\ \mu\mathrm{M}$ [47] and because ribavirin accumulates in plasma to its maximum concentration in ~4 weeks, we set $t_a=5.4\ \mathrm{d}$ [6,38]. The remaining parameter values $k_p=65\ \mathrm{d}^{-1}$, $k_d=0.5\ \mathrm{d}^{-1}$, $C_{50}=408\ \mu\mathrm{M}$, and $\gamma=1$ are obtained from best-fits of our model predictions to experimental data (Fig. 5A). We summarize model parameters and their values in Table 1.

Fits of model predictions to patient data

We fit model predictions to experimental data (Fig. 5A) using the nonlinear regression tool NLINFIT in MATLAB.

Table 1. Summary of model parameters and their values employed.

Parameter	Description	Value (95% CI)[a]	Source
V	Volume of blood	5 L	[67]
v_e	Volume of one RBC	9×10^{-14} L	[67]
t_a	Characteristic timescale of accumulation of RBV in plasma	5.4 d	[6,38]
b	Coefficient determining sensitivity of RBC production rate to changes in number per volume of RBCs	7	[59]
D_0	Death rate of RBCs in the absence of ribavirin	8.3×10^{-3} d^{-1}	[49,66]
Hb_0	Initial Hb level	14.4 g/dL	[47]
$C_p^{\max}$	Steady state plasma RBV concentration	7.5 μM	[47]
θ	RBC population per unit volume at which RBC production rate is half maximal		Determined from pretreatment steady state, $P(0)=D_0N_0$
P_{max}	Maximum production rate of RBCs	8.4×10^{12} cells d^{-1}	Best-fit (Text S3)
k_p	Phosphorylation rate of ribavirin in RBCs	65 (47–84) d^{-1}	Best-fit (Fig. 5A)
k_d	Loss rate of ribavirin phosphorylated analogs in RBCs	0.5 (0.3–0.7) d^{-1}	Best-fit (Fig. 5A)
C_{50}	Concentration of ribavirin phosphorylated analogs at which RBC death rate is twice the pretreatment value	408 (189–628) μM	Best-fit (Fig. 5A)
γ	Coefficient determining sensitivity of RBC death rate to changes in concentration of ribavirin phosphorylated analogs	1 (0.2–1.8)	Best-fit (Fig. 5A)

[a]Typical values employed. Variations are indicated in the text and in figure legends.

doi:10.1371/journal.pcbi.1001072.t001

Supporting Information

Figure S1 Hemoglobin reduction as a function of the intracellular ribavirin concentration.
Found at: doi:10.1371/journal.pcbi.1001072.s001 (0.09 MB PDF)

Figure S2 Analysis of RBC recovery following phlebotomy.
Found at: doi:10.1371/journal.pcbi.1001072.s002 (0.41 MB PDF)

Figure S3 Validation of the solution methodology.
Found at: doi:10.1371/journal.pcbi.1001072.s003 (0.39 MB PDF)

Figure S4 Sensitivity of the numerical solution to the integration time step.
Found at: doi:10.1371/journal.pcbi.1001072.s004 (0.37 MB PDF)

Text S1 Derivation of equation (1) and its boundary condition.
Found at: doi:10.1371/journal.pcbi.1001072.s005 (0.29 MB PDF)

Text S2 Dependence of RBC death rate on intracellular ribavirin concentration.
Found at: doi:10.1371/journal.pcbi.1001072.s006 (0.19 MB PDF)

Text S3 Analysis of phlebotomy experiments.
Found at: doi:10.1371/journal.pcbi.1001072.s007 (0.28 MB PDF)

Text S4 Solution of model equations using the method of characteristics.
Found at: doi:10.1371/journal.pcbi.1001072.s008 (0.30 MB PDF)

Text S5 MATLAB program for solving model equations.
Found at: doi:10.1371/journal.pcbi.1001072.s009 (0.19 MB PDF)

Text S6 Validation of the solution methodology.
Found at: doi:10.1371/journal.pcbi.1001072.s010 (0.20 MB PDF)

Acknowledgments

We thank Alan S. Perelson and Ruy M. Ribeiro for helpful comments.

Author Contributions

Conceived and designed the experiments: SMK NMD. Performed the experiments: SMK. Analyzed the data: SMK NMD. Contributed reagents/materials/analysis tools: SMK NMD. Wrote the paper: SMK NMD.

References

1. Lavanchy D (2009) The global burden of hepatitis C. Liver Int 29: 74–81.
2. Ghany MG, Strader DB, Thomas DL, Seeff LB (2009) Diagnosis, management, and treatment of hepatitis C: An update. Hepatology 49: 1335–1374.
3. Dusheiko G, Main J, Thomas H, Reichard O, Lee C, et al. (1996) Ribavirin treatment for patients with chronic hepatitis C: results of a placebo-controlled study. J Hepatol 25: 591–598.
4. Bodenheimer HC, Lindsay KL, Davis GL, Lewis JH, Thung SN, et al. (1997) Tolerance and efficacy of oral ribavirin treatment of chronic hepatitis C: A multicenter trial. Hepatology 26: 473–477.
5. Zoulim F, Haem J, Ahmed SS, Chossegros P, Habersetzer F, et al. (1998) Ribavirin monotherapy in patients with chronic hepatitis C: a retrospective study of 95 patients. J Viral Hepat 5: 193–198.
6. Pawlotsky JM, Dahari H, Neumann AU, Hezode C, Germanidis G, et al. (2004) Antiviral action of ribavirin in chronic hepatitis C. Gastroenterology 126: 703–714.
7. Manns MP, McHutchison JG, Gordon SC, Rustgi VK, Shiffman M, et al. (2001) Peginterferon alfa-2b plus ribavirin compared with interferon alfa-2b plus ribavirin for initial treatment of chronic hepatitis C: a randomised trial. Lancet 358: 958–965.
8. Fried MW, Shiffman ML, Reddy KR, Smith C, Marinos G, et al. (2002) Peginterferon alfa-2a plus ribavirin for chronic hepatitis C virus infection. N Engl J Med 347: 975–982.
9. McHutchison JG, Gordon SC, Schiff ER, Shiffman ML, Lee WM, et al. (1998) Interferon alfa-2b alone or in combination with ribavirin as initial treatment for chronic hepatitis C. N Engl J Med 339: 1485–1492.
10. Reichard O, Norkrans G, Fryden A, Braconier JH, Sonnerborg A, et al. (1998) Randomized, double-blind, placebo-controlled trial of interferon alpha-2b with and without ribavirin for chronic hepatitis C. Lancet 351: 83–87.
11. Poynard T, Marcellin P, Lee SS, Niederau C, Minuk GS, et al. (1998) Randomized trial of interferon alpha2b plus ribavirin for 48 weeks or for 24 weeks versus interferon alpha2b plus placebo for 48 weeks for treatment of chronic infection with hepatitis C virus. Lancet 352: 1426–1432.
12. Franceschi LD, Fattovich G, Turrini F, Brugnara C, Manzato F, et al. (2000) Hemolytic anemia induced by ribavirin therapy in patients with chronic hepatitis C virus infection: Role of membrane oxidative damage. Hepatology 31: 997–1004.
13. Sulkowski MS (2003) Anemia in the treatment of hepatitis C virus Infection. Clin Infect Dis 37: s315–322.
14. Reddy KR, Shiffman ML, Morgan TR, Zeuzem S, Hadziyannis S, et al. (2007) Impact of ribavirin dose reductions in hepatitis C virus genotype 1 patients completing peginterferon alfa-2a/ribavirin treatment. Clin Gastroenterol Hepatol 5: 124–129.
15. Sulkowski MS, Wasserman R, Brooks L, Ball L, Gish R (2004) Changes in haemoglobin during interferon alpha-2b plus ribavirin combination therapy for chronic hepatitis C virus infection. J Viral Hepat 11: 243–250.
16. Reddy KR, Nelson DR, Zeuzem S (2009) Ribavirin: Current role in the optimal clinical management of chronic hepatitis C. J Hepatol 50: 402–411.
17. Hazode C, Forestier N, Dusheiko G, Ferenci P, Pol S, et al. (2009) Telaprevir and peginterferon with or without ribavirin for chronic HCV infection. N Engl J Med 360: 1839–1850.
18. Lemon SM, McKeating JA, Pietschmann T, Frick DN, Glenn JS, et al. (2010) Development of novel therapies for hepatitis C. Antivir Res 86: 79–92.
19. Zeuzem S (2008) Interferon-based therapy for chronic hepatitis C: current and future perspectives. Nat Clin Pract Gastroenterol Hepatol 5: 610–622.
20. Jain MK, Zoellner C (2010) Role of ribavirin in HCV treatment response: now and in the future. Expert Opin Pharmaco 11: 673–683.
21. Landaverde C, Saab S (2009) Optimizing peginterferon and ribavirin administration in difficult-to-treat patient populations. Curr Hepatitis Rep 8: 43–51.
22. Morello J, Rodriguez-Novoa S, Jimenez-Nacher I, Soriano V (2008) Usefulness of monitoring ribavirin plasma concentrations to improve treatment response in patients with chronic hepatitis C. J Antimicrob Chemother 62: 1174–1180.
23. Schmid M, Kreil A, Jessner W, Homoncik M, Datz C, et al. (2005) Suppression of haematopoiesis during therapy of chronic hepatitis C with different interferon alpha mono and combination therapy regimens. Gut 54: 1014–1020.
24. Tod M, Farcy-Afif M, Stocco J, Boyer N, Bouton VR, et al. (2005) Pharmacokinetic/pharmacodynamic and time-to-event models of ribavirin-induced anaemia in chronic hepatitis C. Clin Pharmacokinet 44: 417–428.
25. DebRoy S, Kribs-Zaleta C, Mubayi A, Cardona-Meléndez GM, Medina-Rios L, et al. (2010) Evaluating treatment of hepatitis C for hemolytic anemia management. Math Biosci 225: 141–155.
26. Dieterich DT, Wasserman R, Brau N, Hassanein TI, Bini EJ, et al. (2003) Once-weekly epoetin alfa improves anemia and facilitates maintenance of ribavirin dosing in hepatitis C virus-infected patients receiving ribavirin plus interferon alfa. Am J Gastroenterol 98: 2491–2499.
27. Afdhal NH, Dieterich DT, Pockros PJ, Schiff ER, Shiffman ML, et al. (2004) Epoetin alfa maintains ribavirin dose in HCV-infected patients: a prospective, double-blind, randomized controlled study. Gastroenterology 126: 1302–1311.
28. Rio RAD, Post AB, Singer ME (2006) Cost-effectiveness of hematologic growth factors for anemia occurring during hepatitis C combination therapy. Hepatology 44: 1598–1606.
29. Homoncik M, Sieghart W, Formann E, Schmid M, Ferenci P, et al. (2006) Erythropoietin treatment is associated with more severe thrombocytopenia in patients with chronic hepatitis C undergoing antiviral therapy. Amer J Gastroenterol 101: 2275–2282.
30. Shiffman ML, Salvatore J, Hubbard S, Price A, Sterling RK, et al. (2007) Treatment of chronic hepatitis C virus genotype 1 with peginterferon, ribavirin, and epoetin alpha. Hepatology 46: 371–379.
31. Falasca F, Ucciferri C, Mancino P, Gorgoretti V, Pizzigallo E, et al. (2010) Use of epoetin beta during combination therapy of infection with hepatitis c virus with ribavirin improves a sustained viral response. J Med Virol 82: 49–56.
32. Feld JJ, Hoofnagle JH (2005) Mechanism of action of interferon and ribavirin in treatment of hepatitis C. Nature 436: 967–972.
33. Parker WB (2005) Metabolism and antiviral activity of ribavirin. Virus Res 107: 165–171.
34. Dixit NM, Perelson AS (2006) The metabolism, pharmacokinetics and mechanisms of antiviral activity of ribavirin against hepatitis C virus. Cell Mol Life Sci 63: 832–842.
35. Neumann AU, Lam NP, Dahari H, Gretch DR, Wiley TE, et al. (1998) Hepatitis C viral dynamics in vivo and the antiviral efficacy of interferon-alpha therapy. Science 282: 103–107.
36. Herrmann E, Lee JH, Marinos G, Modi M, Zeuzem S (2003) Effect of ribavirin on hepatitis C viral kinetics in patients treated with pegylated interferon. Hepatology 37: 1351–1358.
37. Colombatto P, Civitano L, Oliveri F, Coco B, Ciccorossi P, et al. (2003) Sustained response to interferon-ribavirin combination therapy predicted by a model of hepatitis C virus dynamics using both HCV RNA and alanine aminotransferase. Antivir Ther 8: 519–530.

38. Dixit NM, Layden-Almer JE, Layden TJ, Perelson AS (2004) Modelling how ribavirin improves interferon response rates in hepatitis C virus infection. Nature 432: 922–924.
39. Dahari H, Ribeiro RM, Perelson AS (2007) Triphasic decline of hepatitis C virus RNA during antiviral therapy. Hepatology 46: 16–21.
40. Dixit NM (2008) Advances in the mathematical modelling of hepatitis C virus dynamics. J Indian I Sci 88: 37–43.
41. Rong L, Dahari H, Ribeiro RM, Perelson AS (2010) Rapid emergence of protease inhibitor resistance in hepatitis C virus. Sci Transl Med 2: 30ra32.
42. Rong L, Perelson AS (2010) Treatment of hepatitis C virus infection with interferon and small molecule direct antivirals: viral kinetics and modeling. Crit Rev Immunol 30: 131–148.
43. Vlierberghe HV, Delanghe JR, Vos MD, Leroux-Roel G (2001) Factors influencing ribavirin-induced hemolysis. J Hepatol 34: 911–916.
44. Takaki S, Tsubota A, Hosaka T, Akuta N, Someya T, et al. (2004) Factors contributing to ribavirin dose reduction due to anemia during interferon alfa2b and ribavirin combination therapy for chronic hepatitis C. J Gastroenterol 39: 668–673.
45. Balan V, Schwartz D, Wu GY, Muir AJ, Ghalib R, et al. (2005) Erythropoietic response to anemia in chronic hepatitis C patients receiving combination pegylated interferon/ribavirin. Am J Gastroenterol 100: 299–307.
46. Donnerer J, Grahovic M, Stelzl E, Kessler HH, Bankuti C, et al. (2006) Ribavirin levels and haemoglobin decline in early virological responders and non-responders to hepatitis C virus combination therapy. Pharmacology 76: 136–140.
47. Inoue Y, Hommaa M, Matsuzaki Y, Shibata M, Matsumura T, et al. (2006) Erythrocyte ribavirin concentration for assessing hemoglobin reduction in interferon and ribavirin combination therapy. Hepatol Res 34: 23–27.
48. Glue P (1999) The clinical pharmacology of ribavirin. Semin Liv Dis 19: 17–24.
49. Krishnan SM, Dixit NM (2009) Estimation of red blood cell lifespan from alveolar carbon monoxide measurements. Transl Res 154: 15–17.
50. Virtue MA, Furne JK, Ho SB, Levitt MD (2004) Use of alveolar carbon monoxide to measure the effect of ribavirin on red blood cell survival. Am J Hematol 76: 107–113.
51. Fellay J, Thompson AJ, Ge D, Gumbs CE, Urban TJ, et al. (2010) ITPA gene variants protect against anaemia in patients treated for chronic hepatitis C. Nature 464: 405–408.
52. Preston SL, Drusano GL, Glue P, Nash J, Gupta SK, et al. (1999) Pharmacokinetics and absolute bioavailability of ribavirin in healthy volunteers as determined by stable-isotope methodology. Antimicrob Agents Chemother 43: 2451–2456.
53. Endres CJ, Moss AM, Ke B, Govindarajan R, Choi DS, et al. (2009) The role of the equilibrative nucleoside transporter 1 (ENT1) in transport and metabolism of ribavirin by human and wild-type or Ent1-/- mouse erythrocytes. J Pharmacol Exp Ther 329: 387–398.
54. McHutchison JG, Manns MP, Brown RS, Reddy KR, Shiffman ML, et al. (2007) Strategies for managing anemia in hepatitis C patients undergoing antiviral therapy. Am J Gastroenterol 102: 880–889.
55. Mangoni ED, Marrone A, Saviano D, Del Vecchio C, Utili R, et al. (2003) Normal erythropoietin response in chronic hepatitis C patients with ribavirin-induced anemia. Antivir Ther 8: 57–63.
56. Glue P, Rouzier-Panis R, Raffanel C, Sabo R, Gupta SK, et al. (2000) A dose-ranging study of pegylated interferon alfa-2b and ribavirin in chronic hepatitis C. Hepatology 32: 647–653.
57. Jarvis SM, Thorn JA, Glue P (1998) Ribavirin uptake by human erythrocytes and the involvement of nitrobenzylthioinosine-sensitive (es)-nucleoside transporters. Br J Pharmacol 123: 1587–1592.
58. Spivak JL (2000) The blood in systemic disorders. Lancet 355: 1707–1712.
59. Mahaffy JM, Belair J, Mackey MC (1998) Hematopoietic model with moving boundary condition and state dependent delay: applications in erythropoiesis. J Theor Biol 190: 135–146.
60. Veng-Pederson P, Chapel S, Schmidt PRL, Al-Huniti NH, Cook RT, et al. (2002) An integrated pharmacodynamic analysis of erythropoietin, reticulocyte, and hemoglobin responses in acute anemia. Pharm Res 19: 1630–1635.
61. Colijn C, Mackey MC (2005) A mathematical model of hematopoiesis–I. Periodic chronic myelogenous leukemia. J Theor Biol 237: 117–132.
62. Roeder I (2006) Quantitative stem cell biology: computational studies in the hematopoietic system. Curr Opin Hematol 13: 222–228.
63. Crauste F, Pujo-Menjouet L, Génieys S, Molina C, Gandrillon O (2008) Adding self-renewal in committed erythroid progenitors improves the biological relevance of a mathematical model of erythropoiesis. J Theor Biol 250: 322–338.
64. Krzyzanski W, Perez-Ruixo J, Vermeulen A (2008) Basic pharmacodynamic models for agents that alter the lifespan distribution of natural cells. J Pharmacokinet Phar 35: 349–377.
65. Savill NJ, Chadwick W, Reece SE (2009) Quantitative analysis of mechanisms that govern red blood cell age structure and dynamics during anaemia. PLoS Comput Biol 5: e1000416.
66. Berk PD, Berlin NI, Blaschke TF, Bloomer JR, Howe RB (1972) Bilirubin production as a measure of red-cell life-span. J Lab Clin Med 79: 364–378.
67. Beck WS (1991) Hematology. MIT Press, Cambridge, Massachusetts.